Altered Calcium Homeostasis Does Not Explain the Contractile Deficit of Diabetic Cardiomyopathy

Lin Zhang,[1,2] Mark B. Cannell,[1] Anthony R.J. Phillips,[2,3] Garth J.S. Cooper,[2,4] and Marie-Louise Ward[1]

OBJECTIVE—This study examines the extent to which the contractile deficit of diabetic cardiomyopathy is due to altered Ca^{2+} homeostasis.

RESEARCH DESIGN AND METHODS—Measurements of isometric force and intracellular calcium ($[Ca^{2+}]_i$, using fura-2/AM) were made in left ventricular (LV) trabeculae from rats with streptozotocin-induced diabetes and age-matched siblings.

RESULTS—At 1.5 mmol/l $[Ca^{2+}]_o$, 37°C, and 5-Hz stimulation frequency, peak stress was depressed in diabetic rats (10 ± 1 vs. 17 ± 2 mN/mm^2 in controls; $P < 0.05$) with a slower time to peak stress (77 ± 3 vs. 67 ± 2 ms; $P < 0.01$) and time to 90% relaxation (76 ± 7 vs. 56 ± 3 ms; $P < 0.05$). No difference was found between groups for either resting or peak Ca^{2+}, but the Ca^{2+} transient was slower in time to peak (39 ± 2 vs. 34 ± 1 ms) and decay (time constant, 61 ± 3 vs. 49 ± 3 ms). Diabetic rats had a longer LV action potential (APD_{50}, 98 ± 5 vs. 62 ± 5 ms; $P < 0.0001$). Western blotting showed that diabetic rats had a reduced expression of sarco(endo)plasmic reticulum Ca^{2+}-ATPase (SERCA)2a, with no difference in expression of the Na^+/Ca^{2+} exchanger. Immunohistochemistry of LV free wall showed that type I collagen was increased in diabetic rats (diabetic 7.1 ± 0.1%, control 12.7 ± 0.1%; $P < 0.01$), and F-actin content reduced (diabetic 56.9 ± 0.6%; control 61.7 ± 0.4%; $P < 0.0001$) with a disrupted structure.

CONCLUSIONS—We find no evidence to support the idea that altered Ca^{2+} homeostasis underlies the contractile deficit of diabetic cardiomyopathy. The slower action potential and reduced SERCA2a expression can explain the slower Ca^{2+} transient kinetics in diabetic rats but not the contractile deficit. Instead, we suggest that the observed LV remodeling may play a crucial role. ***Diabetes* 57:2158–2166, 2008**

Diabetic cardiomyopathy was first recognized by Rubler et al. (1) in diabetic patients with congestive heart failure but no evidence of coronary atherosclerosis. Prominent defects of diabetic cardiomyopathy include the prolonged duration of contraction and relaxation (Boudina and Abel [2]) and reduced cardiac compliance. The rat with streptozotocin (STZ)-induced type 1 diabetes has been widely used as a model of diabetic myopathy (3). STZ rats manifest a variety of signs of myopathy, including cardiac rhythm disturbances, prolonged contraction and/or slowed relaxation, and decreased contraction strength (4–6). Defects in intracellular Ca^{2+} ($[Ca^{2+}]_i$) homeostasis have been implicated in the impaired mechanical performance of the diabetic heart (7,8). However, there is no consensus in results from studies of intracellular Ca^{2+} homeostasis performed on isolated cardiomyocytes; resting Ca^{2+} has been shown to be decreased (9–11), increased (12,13), or unchanged (14,15). Similarly, the amplitude of the Ca^{2+} transient is reported as decreased (11,16–18), increased (12), or unchanged (19,20). It is possible that this lack of consensus is due to different degrees of disease (diabetic stage) and/or experimental conditions (e.g., different stimulation frequencies and temperatures).

The purpose of this study was to reexamine the extent to which changes in Ca^{2+} homeostasis underlie diabetic cardiomyopathy. To do this, we used left ventricular (LV) tissue at 37°C and stimulation frequencies of 0.1–7 Hz. The latter encompasses rates used in other studies and the normal heart rate for rats in the absence of β-adrenergic stimulation (21). Because LV remodeling is also known to occur in diabetic cardiomyopathy (22,23), we examined extracellular matrix type I and III collagen (the most abundant collagen types in heart tissue [24]) and the thin contractile filament F-actin by immunohistochemistry and confocal microscopy and quantified their distribution and abundance.

RESEARCH DESIGN AND METHODS

All animal use was approved by the University of Auckland animal ethics committee. Chemical reagents were obtained from Sigma unless otherwise stated.

Induction of STZ-induced diabetes. Diabetes was induced by a single injection of STZ (60 mg/kg dissolved in 0.9% saline administered intravenously) in adult male Wistar rats (200–250 g). Control rats received injections of 0.9% saline alone. Blood glucose concentrations were measured 48 h after STZ injection (Advantage II; Roche) and weekly thereafter. Diabetes was diagnosed by a sustained glucose concentration >11 mmol/l. Insulin was not administered, and all animals had free access to food and water.

Physiological measurements. Blood pressure measurements were carried out on conscious animals using a tail-cuff method (MC4000 BP; Hatteras Instruments, Cary, NC) after first habituating animals to the procedure. Eight weeks post-injection, animals were anesthetized (5% halothane initially, maintained at 2% concentration in O_2) and the electrocardiogram (ECG) recorded (PowerLab data acquisition system; ADInstruments, Bella Vista, Australia). QT interval was measured from the beginning of the QRS complex to the end of the T wave, averaged over 6–10 cardiac cycles, and normalized to the square root of RR interval (25).

The day after ECG measurements, the animals were again anesthetized, the hearts removed and immersed in 4°C Krebs-Henseleit buffer (KHB) containing, in millimoles per liter: NaCl (118), KCl (4.75), KH_2PO_4 (1.18), $MgSO_4$ (1.18), $NaHCO_3$ (24.8), and D-glucose (10) with 2,3-butanedione monoxime (5) and $CaCl_2$ (0.5). Hearts were subsequently perfused at room temperature

From the [1]Department of Physiology, Faculty of Medical and Health Sciences, University of Auckland, Auckland, New Zealand; the [2]School of Biological Sciences, Faculty of Science, University of Auckland, Auckland, New Zealand; the [3]Department of Surgery, Faculty of Medical and Health Sciences, University of Auckland, Auckland, New Zealand; and the [4]Department of Medicine, Faculty of Medical and Health Sciences, University of Auckland, Auckland, New Zealand.

Corresponding author: Marie-Louise Ward, m.ward@auckland.ac.nz.

Received 31 January 2008 and accepted 13 May 2008.

Published ahead of print at http://diabetes.diabetesjournals.org on 20 May 2008. DOI: 10.2337/db08-0140.

TABLE 1
General characteristics of control and diabetic rats

	Control rats	Diabetic rats
Body weight (g)	433 ± 12 (23)	237 ± 10 (25)§
Heart weight (g)	1.60 ± 0.07 (24)	1.24 ± 0.05 (24)‡
Tibial length (mm)	42.3 ± 0.4 (13)	38.6 ± 0.6 (16)§
Heart weight:body weight ($\times 10^3$)	3.7 ± 0.1 (23)	5.3 ± 0.2 (21)§
Heart weight:tibial length (g/mm)	0.040 ± 0.002 (13)	0.035 ± 0.002 (13)
Blood glucose (mmol/l)	5.0 ± 0.1 (24)	30.7 ± 0.9 (24)§
Systolic blood pressure (mmHg)	112 ± 3 (16)	121 ± 5 (11)
Heart rate (min^{-1})	376 ± 11 (16)	295 ± 5 (11)§
APD_{50} (ms)	62 ± 5 (6)	98 ± 5 (7)§
APD_{90} (ms)	136 ± 10 (6)	195 ± 9 (7)§

Data are means ± SEM (n). ‡$P < 0.001$ and §$P < 0.0001$, Student's t test.

(KHB, gassed with 95% O_2 and 5% CO_2). Spontaneous action potentials were recorded from LV free wall using glass microelectrodes (tip resistance 4–7 MΩ filled with 3 mol/l KCl) and a Neuroprobe amplifier (Model 1600; A-M Systems, Carlsborg, WA) digitized at 10 kHz and acquired using a PowerLab. Action potential duration (APD) was analyzed using IDL software (IDL research Systems, Boulder, CO). APD_{50} and APD_{90} were measured as the time taken for 50 and 90% repolarization of the action potential, respectively. A small correction for varying heart rate was carried out using the square root of the corresponding RR interval, by means similar to those used for the measurement of the QT interval described above.

Isolation of LV trabeculae. An unbranched cylindrical trabecula was dissected from the left ventricle while the heart was perfused with oxygenated KHB containing 20 mmol/l l 2,3-butanedione monoxime and 0.25 mmol/l $CaCl_2$. The trabecula was then transferred to a Perspex bath on the stage of an inverted microscope (Nikon Diaphot 300; Nikon, Tokyo, Japan) and continuously superfused with oxygenated KHB. One end of the preparation was mounted in a hook extending from a force transducer (AE801; SensorOne, Sausalito, CA), with the other end held in a fine snare protruding from a stainless-steel tube. Following a 30-min stabilization period, the trabecula was field stimulated at 0.1 Hz with 5 ms square-wave pulses (20% above threshold) delivered by a Digitimer D100 (Digitimer, Welwyn Garden City, Hertfordshire, U.K.) and extracellular Ca^{2+} ($[Ca^{2+}]_o$) gradually increased to 1.0 mmol/l. Isometric force was normalized to the trabecula cross-sectional area and expressed as stress. LV trabeculae were not different in either length (diabetic 1.4 ± 0.3 mm, $n = 9$; control 1.5 ± 0.2 mm, $n = 9$) or cross-sectional area (diabetic 0.023 ± 0.008 mm^2, $n = 9$; control 0.017 ± 0.003 mm^2, $n = 9$) between groups.

Trabeculae were loaded with the fluorescent Ca^{2+} indicator fura-2/AM (20 μmol/l) at room temperature for 2 h. On completion of loading, the indicator was washed out and sarcomere length adjusted to 2.1–2.2 μm. Trabeculae were illuminated at 340-, 360-, and 380-nm excitation wavelengths using a spectrophotometric system (Cairn, Faversham, U.K.) and the ratio of the emitted fluorescence with 340- and 380-nm excitation was used as a measurement of $[Ca^{2+}]_i$.

Data were acquired using LabView software (National Instruments, Austin, TX) and analyzed offline. Unbiased measurement of Ca^{2+} transient and force was made from data averaged over 7–10 cardiac cycles, using a custom analysis program written in IDL. A five-parameter function was used to define the properties of the averaged Ca^{2+} transient, as previously described (21).

Western blotting. Frozen LV tissue was homogenized in ice-cold lysis buffer (50 mmol/l Tris-HCl, pH 8; 150 mmol/l NaCl; 1% NP-40; 0.5% sodium deoxycholate; and 0.1% sodium dodecylsulphate) with a proteinase inhibitor cocktail (Roche, Indianapolis, IN) and then centrifuged at 13,000*g* for 1 h at 4°C. Protein concentration in the supernatant was determined with a bicinchoninic acid protein assay (Pierce, Rockford, IL). A total of 20 μg protein was used for Western blots using rabbit anti-NCX antibody (Ab) (1:500; Swiss Antibodies, Swant, Switzerland) and mouse anti–sarco(endo)plasmic reticulum Ca^{2+}-ase (SERCA)2a Ab (1:1,000; Affinity BioReagents, Golden, CO). Specific binding was detected with a donkey anti-rabbit or anti-mouse IgG–horseradish peroxidase conjugate (GE Healthcare, Buckinghamshire, U.K.) and ECL Plus Western blotting detection reagents (GE Healthcare) according to the manufacturer's instructions. An LA 3,000 image reader (Fuji Photo Film, Tokyo, Japan) was used to detect signals and take images of the membranes. Images were analyzed using Multi Gauge software (Fuji Photo Film).

Immunohistochemistry. Tissue for immunohistochemistry, frozen at −80°C, was sectioned at 30 μm. The sections were dried (1 h), fixed (ice-cold acetone, 10 min), and rehydrated (PBS, 5 min). Sections were then blocked (60 min, 10% goat serum in PBS) and immunolabeled (4°C) with rabbit anti-rat type I and type III collagen Ab (1:100 in 5% goat serum/1% BSA/PBS; Chemicon, Boronia, Australia). After washing (PBS), slides were stained for 2 h with secondary Abs (1:200) (Alexa Fluor 488 goat anti-rabbit Ab; Invitrogen) and phalloidin-rhodamine (1:50–100, Invitrogen) diluted in 5% goat serum/1% BSA/PBS at room temperature. Slides were washed (PBS), mounted (antifade; Dako), and imaged with a confocal microscope (Zeiss LSM410). Three transverse optical sections from the LV wall adjacent to the endocardium were analyzed from each animal ($n = 7$, per group). F-actin and collagen (types I and III) were quantified using Image J (http://rsb.info.nih.gov/ij) and a custom-written IDL program based on signal thresholding. Results (means ± SEM) were expressed as percentage of cross-sectional area. Differences between means were analyzed using either ANOVA or Student's t test, as appropriate, and were considered significant at $P < 0.05$.

RESULTS

The general characteristics of diabetic rats compared with their age-matched control counterparts are shown in Table 1. Diabetes was confirmed by a significant (approximately sixfold) elevation in blood glucose, 3 days after STZ injection, that was maintained. Eight weeks post-injection, diabetic rats had decreased body weight, tibial length, and heart weight, but their heart weight–to–body weight ratio was increased. In contrast, heart weight normalized to tibial length was not different between groups (Table 1).

Analysis of ECG and LV action potential duration. Diabetic rats had a slower heart rate under anesthesia and a prolonged QT interval both before and after normalization for heart rate (diabetic 192 ± 4 ms, $n = 18$; control 177 ± 4 ms, $n = 11$; $P < 0.05$). Consistent with the longer QT interval, the LV action potential was also prolonged in diabetic rats. These results are summarized in Table 1.

Measurements of intracellular Ca^{2+} and isometric force. Intracellular $[Ca^{2+}]_i$ (fura-2 340/380 ratio) and isometric force were measured in LV trabeculae under experimental conditions that mimicked those in vivo (1.5 mmol/l $[Ca^{2+}]_o$, 37°C, and 5 Hz). Figure 1*A* shows five consecutive cardiac cycles recorded from representative control (solid lines) and diabetic (dotted lines) trabeculae, superimposed for comparison. Parameters describing these data are summarized in Table 2. No difference was found in peak or resting $[Ca^{2+}]_i$ between groups, but the kinetics of the Ca^{2+} transient were slower for diabetic rats (increased time to peak $[Ca^{2+}]_i$ and time constant of Ca^{2+} transient decay; $P < 0.05$). In comparison with their control counterparts, diabetic rats had decreased peak and developed stress with a slower time course (increased time to peak stress and time to 90% relaxation of stress; $P < 0.05$). Figure 1*B* shows superimposed Ca^{2+} transients (i), twitches (ii), and phase plots (iii), obtained by combining averaged data from seven trabeculae per group. The $[Ca^{2+}]_i$-stress relationship (Fig. 1*B*iii) shows a right-shifted

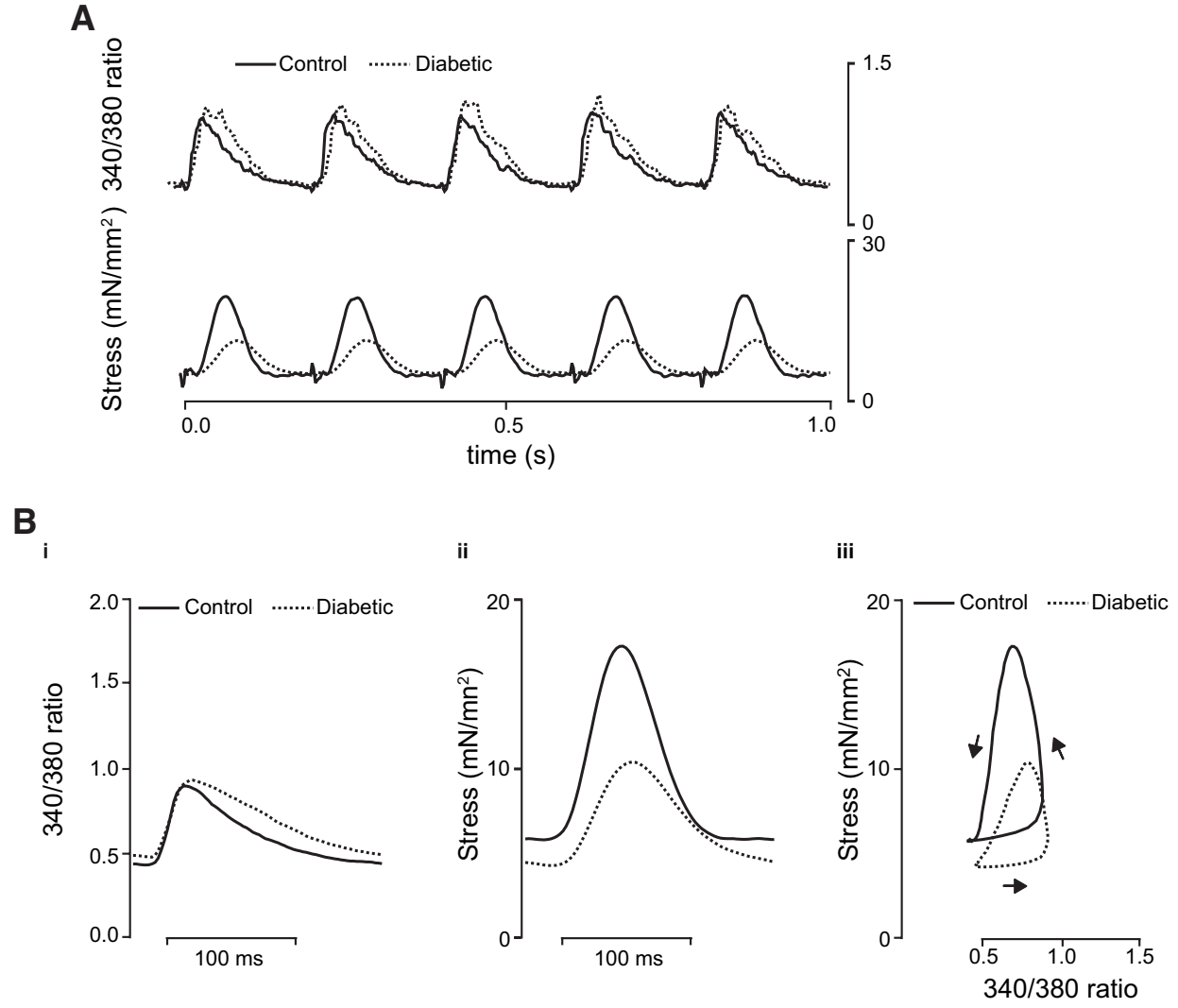

FIG. 1. Data from diabetic (dotted lines) and control (solid lines) rats at 5 Hz, 37°C, and 1.5 mmol/l $[Ca^{2+}]_o$ superimposed for comparison. *A*: Representative traces of fluorescence (340/380 ratio) and force. *B*: Average data from 7 trabeculae per group. Ca^{2+} transient (*i*), stress (*ii*), and phase plane analysis of the relationship between fluorescence and stress during twitch (*iii*). Arrows indicate the direction of time.

relaxation phase for diabetic rats with decreased slope (diabetic 29 ± 7 mN mm^{-2}/ratio unit, $n = 8$; control 67 ± 17 mN mm^{-2}/ratio unit, $n = 8$; $P < 0.05$), suggesting that myofibrillar Ca^{2+} sensitivity was reduced.

Effect of $[Ca^{2+}]_o$ on $[Ca^{2+}]_i$ and stress. Increased cytoplasmic Ca^{2+} can paradoxically reduce sarcoplasmic reticulum (SR) Ca^{2+} content when it increases the probability and frequency of spontaneous Ca^{2+} release from the SR during diastole (26,27). This is an important factor for in vitro studies in the rat, as it has been reported that the rat is highly dependent on SR Ca^{2+} stores for contraction (28) and susceptible to spontaneous SR diastolic Ca^{2+}

TABLE 2
Intracellular Ca^{2+} and mechanical stress (for 1.5 mmol/l $[Ca^{2+}]_o$, 5 Hz, 37°C)

	Control rats	Diabetic rats
Peak 340/380 ratio	1.1 ± 0.1 (10)	1.2 ± 0.2 (7)
Resting 340/380 ratio	0.41 ± 0.05 (10)	0.45 ± 0.1 (7)
Time to peak fluorescence (ms)	34 ± 1 (9)	39 ± 2 (7)*
Time constant of fluorescence decay (ms)	49 ± 3 (9)	61 ± 3 (7)†
Maximum rate of rise of 340/380 ratio (s^{-1})	24 ± 3 (9)	21 ± 3 (7)
Peak stress (mN/mm^2)	17 ± 2 (9)	10 ± 1 (8)†
Resting stress (mN/mm^2)	5 ± 1 (9)	4 ± 1 (8)
Time to peak stress (ms)	67 ± 2 (9)	77 ± 3 (9)*
Time to 50% relaxation (ms)	32 ± 1 (9)	42 ± 4 (9)†
Time to 90% relaxation (ms)	56 ± 3 (9)	76 ± 7 (9)†
Maximum rate of rise of stress (mN/mm^2 per s)	350 ± 60 (9)	180 ± 20 (9)†

Data are means ± SEM (n). *$P < 0.01$ and †$P < 0.05$, Student's t test.

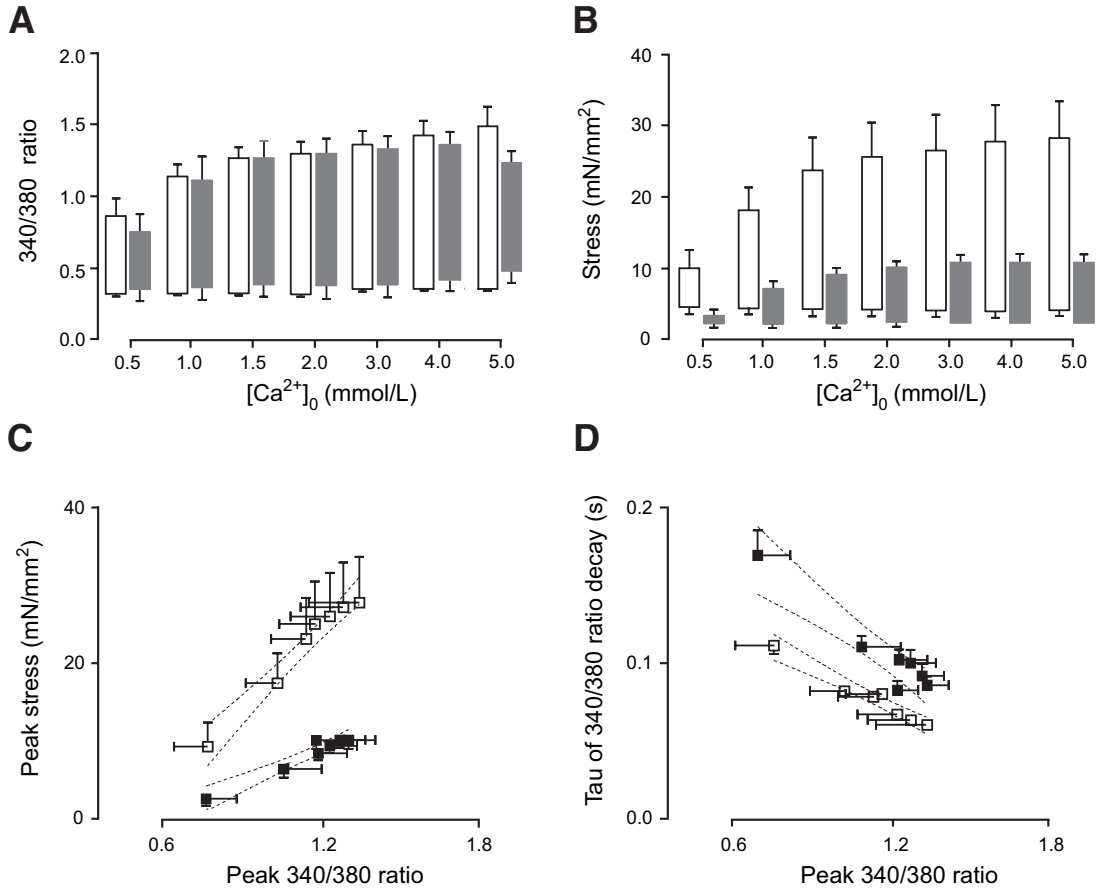

FIG. 2. The effect of $[Ca^{2+}]_o$ on fluorescence and stress at 0.1 Hz and 37°C. Solid bars and symbols show data from diabetic rats ($n = 6$); open bars and symbols are matched controls ($n = 6$). *A*: Effect of $[Ca^{2+}]_o$ on peak and resting fluorescence. *B*: Effect of $[Ca^{2+}]_o$ on resting, developed, and peak stress. *C*: Relationship between peak fluorescence and peak stress. Control rats: $R^2 = 0.97$, slope = 33.9. Diabetic rats: $R^2 = 0.94$, slope = 14.49. *D*: Effect of $[Ca^{2+}]_o$ on time constant (tau) of fluorescence decay. Control rats: $R^2 = 0.96$, slope −0.086. Diabetic rats: $R^2 = 0.94$, slope −0.125; $P < 0.05$. Data are means ± SEM. Linear regression analysis was made from mean values, and dotted lines show the 95% CIs.

release (27). To examine the possibility that this effect might be altering Ca^{2+} release, trabeculae were exposed to a range of extracellular Ca^{2+} concentrations from 0.5 to 5 mmol/l. There was no difference between groups for either resting $[Ca^{2+}]_i$ (Fig. 2*A*) or resting stress (Fig. 2*B*) at all $[Ca^{2+}]_o$. Although peak $[Ca^{2+}]_i$ and peak stress increased with increasing $[Ca^{2+}]_o$ in both groups, peak stress was reduced in diabetic animals at all $[Ca^{2+}]_o$ ($P < 0.05$; Fig. 2*A* and *B*). In contrast, there was no difference in peak $[Ca^{2+}]$ between groups, consistent with the lack of a difference in resting $[Ca^{2+}]_i$.

Figure 2*C* examines the relationship between peak $[Ca^{2+}]_i$ and peak stress and clearly shows that, regardless of the peak $[Ca^{2+}]_i$, diabetic rats had decreased responsiveness to $[Ca^{2+}]_i$. It is well known that the time course of the Ca^{2+} transient affects force responses and that a decrease in the duration of the transient decreases force. Figure 2*C* shows that regardless of the peak $[Ca^{2+}]_i$ reached, diabetic trabeculae developed less stress, whereas Fig. 2*D* shows that they also had a slower Ca^{2+} transient (which would be expected to increase force production [29]). The reduced slope of the relationship between peak $[Ca^{2+}]_i$ and peak force (Fig. 2*C*) is consistent with diabetic rats having a diminished myofibrillar Ca^{2+} sensitivity.

Effect of stimulation frequency on $[Ca^{2+}]_i$ and stress. In cardiac muscle, force is also modulated by stimulation frequency, and as noted above, most in vitro investigations have been carried out at low stimulation frequencies. We examined the response of trabeculae to stimulation frequencies in the range 0.1–7 Hz (Fig. 3). Trabeculae from control rats ($n = 6$) showed a biphasic response for developed stress and Ca^{2+}transient amplitude with increasing stimulation frequency (Figs. 3*A* and 3*B*). There were no differences in peak or resting $[Ca^{2+}]_i$ between diabetic and control rats, except at 7 Hz, where resting $[Ca^{2+}]_i$ was increased in diabetic animals (Fig. 3*A*). The positive phase of the force-frequency response was diminished in diabetic rats ($n = 6$; Fig. 3*B*) such that, despite the increase in the Ca^{2+} transient with frequency, force did not follow. Both diabetic and control rats showed frequency-dependent acceleration in the decay of the Ca^{2+} transient (Fig. 3*C*) and force relaxation (Fig. 3*D*), but these parameters were always slower for diabetic rats ($P < 0.05$).

Taken together, these results show that the reduced contractility of diabetic rat hearts cannot be explained on the basis of an altered $[Ca^{2+}]_i$, although there were changes in Ca^{2+} homeostasis that slowed the Ca^{2+} transient.

Western blotting. The rate of decline of the Ca^{2+} transient is dominated by the rate of Ca^{2+} uptake by the SR and, to a lesser extent, sarcolemmal Ca^{2+} extrusion by the Na^+/Ca^{2+} exchanger (NCX), which contributes ~15% (30). Figure 4 shows Western blots of SERCA2a and NCX protein expression. Diabetic rats had lower levels of

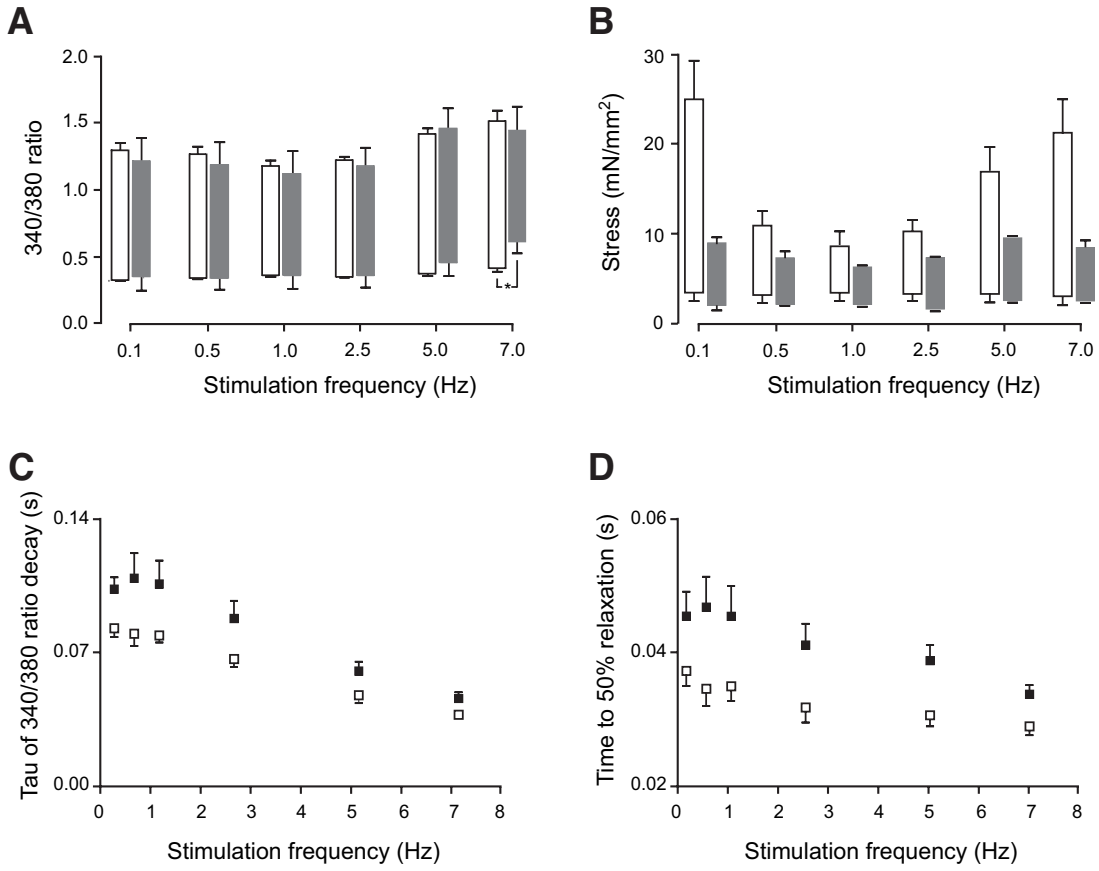

FIG. 3. The effect of stimulation frequency on fluorescence and stress at 1.5 mmol/l $[Ca^{2+}]_o$ and 37°C. Solid bars and symbols show data from diabetic rats ($n = 6$); open bars and symbols show data from matched controls ($n = 6$). *A*: Peak fluorescence was not different between groups and showed a biphasic response to increasing stimulation frequency. No effect of stimulation frequency was found between groups for resting fluorescence, apart from at 7 Hz, where it was increased in diabetic rats. *B*: Resting, developed, and peak stress in response to stimulation frequency. *C*: Time constant (tau) of fluorescence decay in response to stimulation frequency. *D*: Time to 50% relaxation in response to stimulation frequency. Control rats: $R^2 = 0.99$, slope −0.007. Diabetic rats: $R^2 = 0.97$, slope −0.009. Data are means ± SEM. *$P < 0.05$ compared between groups.

SERCA2a expression ($P < 0.05$), whereas NCX was not significantly altered. This result suggests that the origin of the slowed Ca^{2+} transient in diabetic hearts resides in a decrease in the SR uptake capacity.

Immunohistochemistry of type I and type III collagen and F-actin. Because cardiac remodeling may contribute to diabetic cardiomyopathy (23,24), we examined the extracellular collagen content and the organization of sarcomeric thin filaments (F-actin). Figure 5 shows images of typical antibody-labeling patterns for type I collagen (green) and phalloidin-labeled F-actin (red) in diabetic and control rats. Diabetic hearts showed increased type I collagen per endocardial cross-sectional area (diabetic 7.1 ± 0.1% of area, control 6.2 ± 0.2% of area; $P < 0.01$) without significant change in type III collagen (diabetic 6.5 ± 0.1% of area, control: 6.2 ± 0.1% of area). Diabetic rats also showed a more disorganized F-actin structure with decreased F-actin content (diabetic 56.9 ± 0.6% of area, control 61.7 ± 0.4% of area; $P < 0.0001$).

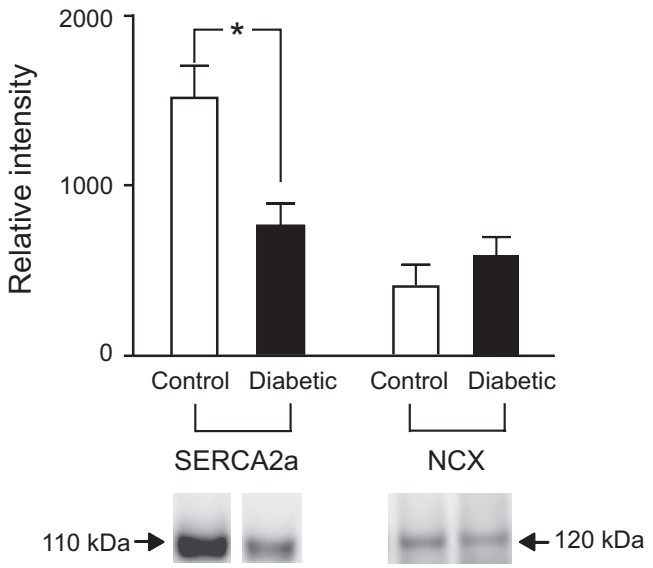

FIG. 4. LV free wall tissue expression of the SR Ca^{2+}-ATPase (SERCA2a, $n = 8$) and Na^+/Ca^{2+} exchanger (NCX, $n = 7$) protein. In comparison to control rats (□), diabetic rats (■) showed reduced expression of SERCA2a, with no change of NCX expression. Data are means ± SEM. *$P < 0.05$ compared between groups.

DISCUSSION

Diabetic cardiomyopathy or "diabetic heart muscle disease" starts as an asymptomatic slowing in relaxation kinetics (diastolic dysfunction) (31). As the syndrome progresses, systolic function also becomes compromised, which increases morbidity and mortality (32). In the present study, STZ-injected rats were used as a model of

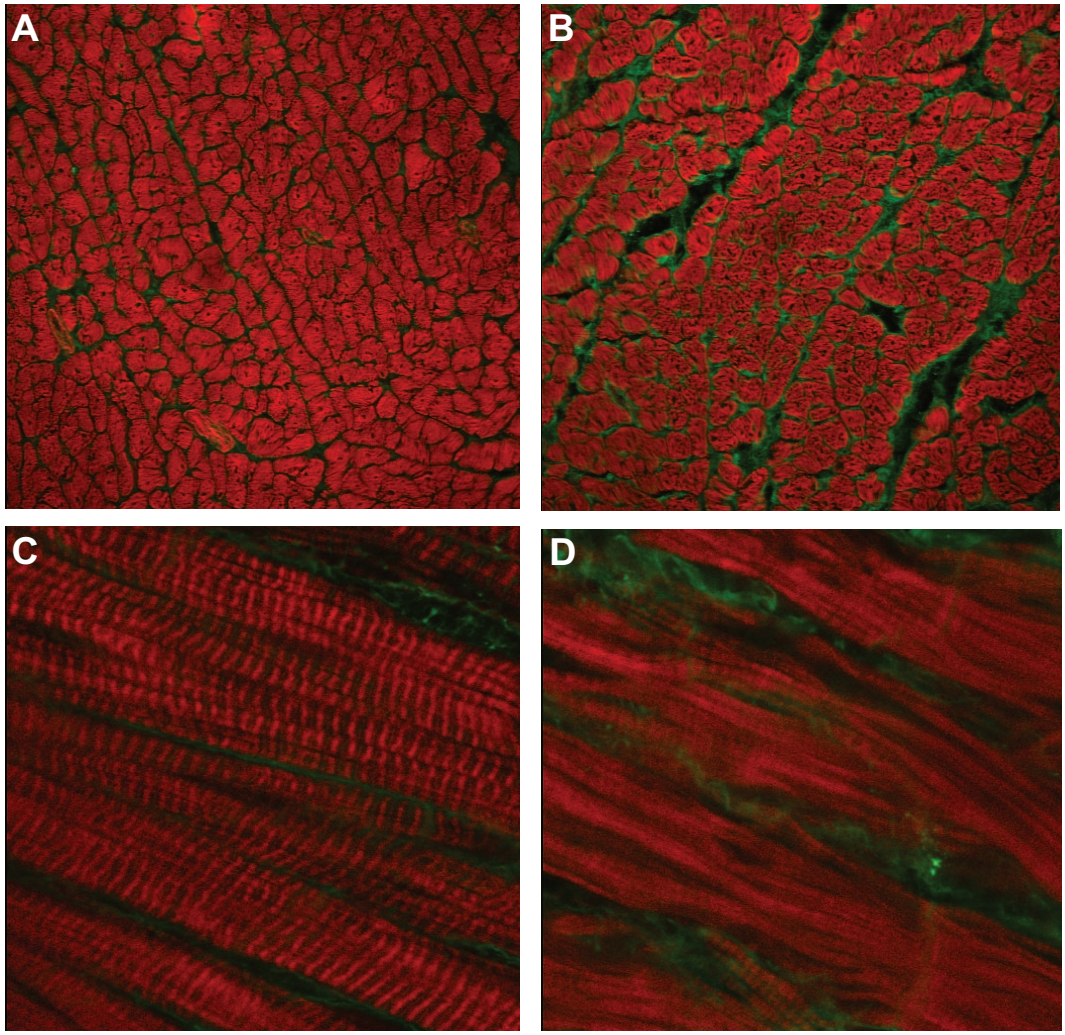

FIG. 5. Representative confocal images of LV free wall immunolabelled for type 1 collagen (green) and F-actin (red). *A* and *B*: Cross-section from endocardium (×25 objective, zoom ×3) from control (*A*) and diabetic (*B*) rats. *C* and *D*: Longitudinal sections (63× objective, zoom ×3) from control (*C*) and diabetic (*D*) rats. (Please see http://dx.doi.org/10.2337/db08-0140 for a high-quality digital representation of this figure.)

diabetic cardiomyopathy (8) and cardiac function, evaluated in relation to cellular $[Ca^{2+}]_i$ homeostasis, electrical activity, and remodeling of the left ventricle.

Diabetic rats had a decreased heart rate with depressed SR Ca^{2+}-uptake capacity and no detectable change in NCX. Although the cause of the decreased SA node discharge rate was not examined, our data suggest a possible explanation. SA nodal cell action potential generation is promoted by spontaneous SR Ca^{2+} release, which produces inward current by NCX (Maltsev et al. [33]). In our model, a reduced ability of the SR to take up Ca^{2+} might delay the time taken for the SR to reach the level of Ca^{2+} that promotes spontaneous release. This would therefore reduce SA nodal cell discharge rate, as observed.

At 1.5 mmol/l $[Ca^{2+}]_o$, 37°C, and 5 Hz, which are close to physiological conditions, trabeculae from diabetic rats showed depressed contractility with prolonged time for contraction and relaxation (Table 2). This result is consistent with previous studies from our group using the isolated working heart (34) and from other research groups, albeit under different conditions (8,17,35). Altered intracellular Ca^{2+} homeostasis has previously been suggested as underlying diabetic cardiac dysfunction (Pierce and Russell [7] and Cesario et al. [36]) although, as noted, results are inconsistent. Although some of these discrepancies might be attributable to the extent of disease progression (diabetic stage) and experimental conditions, few studies have examined $[Ca^{2+}]_i$ and the control of contractility under near-physiological temperatures and rates of stimulation. This problem is illustrated in Fig. 3; at 1 and 2.5 Hz, there was no detectable difference in developed stress between groups, despite contractility being very much reduced at all other frequencies tested in diabetic rats. In the present study, experiments were performed from a base of 37°C and 5 Hz, and our data showed that diabetic rats had an unchanged resting $[Ca^{2+}]_i$ level, maximum rate of rise in fluorescence, and Ca^{2+} transient amplitude, despite showing reduced contractility. These results are consistent with some previous studies (14,15) performed on isolated cardiomyocytes at 35–37°C and 1 Hz. In contrast, results from other studies showed a reduced Ca^{2+} transient amplitude or peak $[Ca^{2+}]_i$ (11,16–18), but it should be noted that those experiments were performed at low temperature (21–25°C) and low stimulation frequencies (0.2–0.5 Hz).

Our results also showed that diabetic rats had prolonged time to peak $[Ca^{2+}]_i$ and prolonged time constant of Ca^{2+} transient decay (Table 2), consistent with some other studies (6,11,14–16). Although the time to peak $[Ca^{2+}]_i$ was slower, the rate of rise of the Ca^{2+} transient was not

significantly altered. The latter observation suggests that the trigger for Ca^{2+} release (I_{Ca}) was not reduced, with the delayed peak of the Ca^{2+} transient likely due to the prolonged action potential duration. The reduction in the level of expression of SERCA2a (~50%), as detected by Western blots (Fig. 4), appears sufficient to explain the reduction (~20%) in the rate of decline of the Ca^{2+} transient. The slower kinetics of the Ca^{2+} transient would contribute to the prolonged time course of cardiac contraction and relaxation in diabetic rats, but it is unclear whether the reduced rate of the decay in the Ca^{2+} transient is sufficient to explain the slowed mechanical relaxation. By comparing contractions between normal and diabetic rats at different stimulation rates, we can select contractions that have similar rates of Ca^{2+} transient decline to isolate the effect on contraction. For example, at 5 Hz, the diabetic rat Ca^{2+} transient decreases slightly faster than that of the control rat at 2.5 Hz (Fig. 3*C*). However, the time to 90% mechanical relaxation of the diabetic rat at 5 Hz (Table 2) is about 80 ms, whereas that of the control rat takes about 60 ms at 2.5 Hz. Similarly, for 50% mechanical relaxation, the times were 39 ms and 32 ms (for diabetic rats at 5 Hz and control rats at 2.5 Hz, respectively). From these comparisons, we suggest that the mechanical relaxation is intrinsically slower in diabetic animals and exacerbated by the reduced rate of decrease of $[Ca^{2+}]_i$. In support of this idea, we also observed an increase in the time to peak stress in diabetic rats over and above that expected from the delayed time to peak $[Ca^{2+}]_i$.

The slower kinetics of the Ca^{2+} transient in diabetic rats may also be affected by the prolonged APD (Table 1), altered intracellular Ca^{2+} handling, or the combination of both. It is well known that maintained depolarization slows the return of $[Ca^{2+}]_i$ to resting levels (37), an effect that is partly due to inhibition of Ca^{2+} extrusion by NCX. On the other hand, slowed SR Ca^{2+} uptake should lead to prolonged depolarization due to inward current generation by forward-mode NCX. The latter explanation seems likely because we found decreased levels of SERCA2a expression in the diabetic rat. Decreased SERCA2a expression should alter the balance of Ca^{2+} homeostasis in favor of increased Ca^{2+} extrusion via NCX and might be expected to reduce SR Ca^{2+} content. However, Ca^{2+} extrusion via NCX during the decline of the Ca^{2+} transient will lead to Na^+ entry, which, during the diastolic period, will increase resting $[Ca^{2+}]_i$ and help restore SR Ca^{2+} levels. This is consistent with our observation of a slightly increased resting $[Ca^{2+}]_i$ in diabetic rats (at least at 0.1 Hz and varied $[Ca^{2+}]_o$), although detailed modeling will be required to determine whether the change in SR Ca^{2+} uptake is by itself sufficient to explain all the effects on the APD and resting $[Ca^{2+}]_i$.

Although we found almost no effects on peak Ca^{2+} in a variety of conditions, the finding that there was a reduced rate of SR Ca^{2+} uptake and SERCA2a expression was surprising, since these changes might be expected to decrease SR Ca^{2+} content (and therefore the amplitude of the Ca^{2+} transient). Simple interpretation of changes in Ca^{2+} transient kinetics is complicated by the interaction of some Ca^{2+} transport mechanisms with changes in membrane potential during the action potential. To separate these two effects, a logarithmic analysis of the decline of the Ca^{2+} transient is shown in Fig. 6. It is clear that there is a delay before the decline of fluorescence becomes exponential. It is notable that this delay is longer in

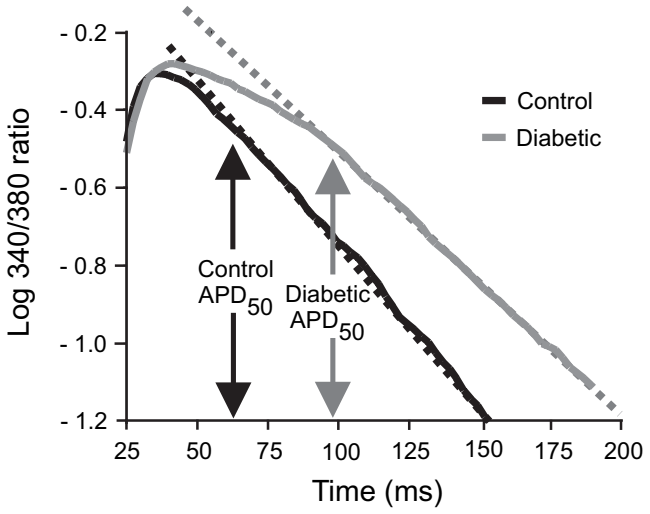

FIG. 6. Logarithmic plot of averaged 340/380 ratio from diabetic (n = 7) and control (n = 7) rat trabeculae. Dotted lines fitted to each curve indicate the linear portion of the response. Note that the decay in fluorescence becomes linear at approximately the APD_{50} for each group but is delayed in diabetic rats.

diabetic rats and that the duration corresponds closely to the time for 50% action potential repolarization. After the delay, the rate of decline of the Ca^{2+} transient was slower in diabetic rats, as described above. The slowed initial phase of the decrease in the Ca^{2+} transient must be due to either continued sarcolemmal Ca^{2+} influx or a failure for SR release to terminate (because $dCa_i/dt = J_{influx} - J_{efflux}$). The latter factor would also be expected to reduce SR Ca^{2+} content, but because the amplitude of the Ca^{2+} transient was not reduced, increased sarcolemmal Ca^{2+} influx during this period seems more likely. Because the 50% repolarization potential corresponds to a time when Ca^{2+} influx via L-type Ca^{2+} channels terminates (38), the increased duration of the diabetic action potential would be expected to increase Ca^{2+} influx and may therefore explain why the Ca^{2+} is not decreased, in spite of a decreased SR uptake capacity.

Phospholamban is an endogenous inhibitor of SERCA activity in cardiac muscle, especially at low $[Ca^{2+}]_i$, and might contribute to the differences in the decay of the transient between groups. However, the inhibitory effects of phospholamban are calcium dependent; as $[Ca^{2+}]_i$ is increased, the effects are diminished. Figs. 2*D* and 3*D* show the time constant of Ca^{2+} decay as a function of the peak fluorescence for both diabetic and control trabeculae under experimental conditions that alter $[Ca^{2+}]_i$. Linear regression analysis for both datasets (Figs. 2*D* and 3*D*) showed that the slopes of the regression lines were either steeper (Fig. 2*D*) or not different (Fig. 3*D*) for diabetic hearts, suggesting that decreased phospholamban does not explain the slower decay of $[Ca^{2+}]_i$ in diabetic hearts.

Diabetic rats showed depressed cardiac contractility, even when peak $[Ca^{2+}]_i$ was matched by altering stimulation rate (Fig. 3*A* and 3*B*), suggesting that altered $[Ca^{2+}]_i$ handling was not the primary cause of contractile dysfunction. Because depressed cardiac myofibrillar ATPase activity occurs in diabetic cardiomyopathy (39), it might seem obvious to attribute the contractile dysfunction to this effect. However, we also observed a ~8% reduction in the fractional area of actin filament (F-actin) per unit cross-section that will also contribute to a reduction in active stress. The reduced F-actin labeling per cross-

section may be explicable on the basis of decreased protein synthesis, increased protein degradation (40), and reduced α-actin mRNA expression (41). More importantly, F-actin no longer showed a highly organized sarcomeric distribution in diabetic hearts (Fig. 5*D*). Activation of cardiac muscle myofilaments involves a series of complex interactions between the troponin complex, tropomyosin, and F-actin. The contractile deficit might therefore arise, in part, from an overall reduction in the number of myosin-binding sites available for crossbridge formation. Additionally, changes to the sarcomeric organization of F-actin might also explain the reduced myofilament Ca^{2+} sensitivity in diabetic trabeculae.

Diabetic cardiomyopathy is also associated with increased stiffness in the left ventricle (42). Types I and III collagen are the most abundant collagen types in the heart, forming 85 and 11% of the total collagen content, respectively (24). Our results show an increase (14%) in type I collagen in diabetic rats but no change in type III. However, any diastolic dysfunction arising from increased collagen would be compounded by the reduced rate of decline of the Ca^{2+} transient and its effects on force production.

In summary, under physiological conditions, we find no evidence to support the idea that altered myocardial Ca^{2+} handling underlies the decrease in contractile force in diabetic cardiomyopathy. Although decreased SR Ca^{2+} uptake exists, it is offset by an increase in action-potential duration, thereby ensuring that SR Ca^{2+} content is maintained. Instead, our data indicate that the contractile function is compromised by reduced and disrupted F-actin in conjunction with the increased type I collagen. In addition, we found evidence for a decreased myofilament sensitivity and slowed relaxation independent of the changes in the Ca^{2+} transient. Although the contribution of the observed structural changes to the contractile deficit in the diabetic heart cannot be evaluated at this time, such changes deserve careful consideration in future studies.

ACKNOWLEDGMENTS

This work was supported by the Health Research Council of New Zealand.

REFERENCES

1. Rubler S, Dlugash J, Yuceoglu YZ, Kumral T, Branwood AW, Grishman A: New type of cardiomyopathy associated with diabetic glomerulosclerosis. *Am J Cardiol* 30:595–602, 1972
2. Boudina S, Abel ED: Diabetic cardiomyopathy revisited. *Circulation* 115:3213–3223, 2007
3. Rees DA, Alcolado JC: Animal models of diabetes mellitus. *Diabet Med* 22:359–370, 2005
4. Howarth FC, Jacobson M, Naseer O, Adeghate E: Short-term effects of streptozotocin-induced diabetes on the electrocardiogram, physical activity and body temperature in rats. *Exp Physiol* 90:237–245, 2005
5. Shimoni Y, Firek L, Severson D, Giles W: Short-term diabetes alters K^+ currents in rat ventricular myocytes. *Circ Res* 74:620–628, 1994
6. Magyar J, Rusznak Z, Szentesi P, Szucs G, Kovacs L: Action potentials and potassium currents in rat ventricular muscle during experimental diabetes. *J Mol Cell Cardiol* 24:841–853, 1992
7. Pierce GN, Russell JC: Regulation of intracellular Ca^{2+} in the heart during diabetes. *Cardiovasc Res* 34:41–47, 1997
8. Choi KM, Zhong Y, Hoit BD, Grupp IL, Hahn H, Dilly KW, Guatimosim S, Lederer WJ, Matlib MA: Defective intracellular Ca^{2+} signaling contributes to cardiomyopathy in type 1 diabetic rats. *Am J Physiol Heart Circ Physiol* 283:H1398–H1408, 2002
9. Norby FL, Wold LE, Duan J, Hintz KK, Ren J: IGF-I attenuates diabetes-induced cardiac contractile dysfunction in ventricular myocytes. *Am J Physiol Endocrinol Metab* 283:E658–E666, 2002
10. Ozdemir S, Ugur M, Gurdal H, Turan B: Treatment with AT(1) receptor blocker restores diabetes-induced alterations in intracellular Ca^{2+} transients and contractile function of rat myocardium. *Arch Biochem Biophys* 435:166–174, 2005
11. Yaras N, Ugur M, Ozdemir S, Gurdal H, Purali N, Lacampagne A, Vassort G, Turan B: Effects of diabetes on ryanodine receptor Ca release channel (RyR_2) and Ca^{2+} homeostasis in rat heart. *Diabetes* 54:3082–3088, 2005
12. Howarth FC, Adem A, Adeghate EA, Al Ali NA, Al Bastaki AM, Sorour FR, Hammoudi RO, Ghaleb NA, Chandler NJ, Dobrzynski H: Distribution of atrial natriuretic peptide and its effects on contraction and intracellular calcium in ventricular myocytes from streptozotocin-induced diabetic rat. *Peptides* 26:691–700, 2005
13. Howarth FC, Qureshi MA: Effects of carbenoxolone on heart rhythm, contractility and intracellular calcium in streptozotocin-induced diabetic rat. *Mol Cell Biochem* 289:21–29, 2006
14. Howarth FC, Qureshi A, Singh J: Effects of acidosis on ventricular myocyte shortening and intracellular Ca^{2+} in streptozotocin-induced diabetic rats. *Mol Cell Biochem* 261:227–233, 2004
15. Howarth FC, Qureshi MA, White E: Effects of hyperosmotic shrinking on ventricular myocyte shortening and intracellular Ca^{2+} in streptozotocin-induced diabetic rats. *Pflugers Arch* 444:446–451, 2002
16. Kotsanas G, Delbridge LM, Wendt IR: Stimulus interval-dependent differences in Ca^{2+} transients and contractile responses of diabetic rat cardiomyocytes. *Cardiovasc Res* 46:450–462, 2000
17. Noda N, Hayashi H, Satoh H, Terada H, Hirano M, Kobayashi A, Yamazaki N: Ca^{2+} transients and cell shortening in diabetic rat ventricular myocytes. *Jpn Circ J* 57:449–457, 1993
18. Lagadic-Gossmann D, Buckler KJ, Le Prigent K, Feuvray D: Altered Ca^{2+} handling in ventricular myocytes isolated from diabetic rats. *Am J Physiol* 270:H1529–H1537, 1996
19. Yu JZ, Rodrigues B, McNeill JH: Intracellular calcium levels are unchanged in the diabetic heart. *Cardiovasc Res* 34:91–98, 1997
20. Singh J, Chonkar A, Bracken N, Adeghate E, Latt Z, Hussain M: Effect of streptozotocin-induced type 1 diabetes mellitus on contraction, calcium transient, and cation contents in the isolated rat heart. *Ann N Y Acad Sci* 1084:178–190, 2006
21. Ward ML, Pope AJ, Loiselle DS, Cannell MB: Reduced contraction strength with increased intracellular $[Ca^{2+}]$ in left ventricular trabeculae from failing rat hearts. *J Physiol* 546:537–550, 2003
22. Nemoto O, Kawaguchi M, Yaoita H, Miyake K, Maehara K, Maruyama Y: Left ventricular dysfunction and remodeling in streptozotocin-induced diabetic rats. *Circ J* 70:327–334, 2006
23. Reddi AS: Collagen metabolism in the myocardium of normal and diabetic rats. *Exp Mol Pathol* 48:236–243, 1988
24. Weber KT: Cardiac interstitium in health and disease: the fibrillar collagen network. *J Am Coll Cardiol* 13:1637–1652, 1989
25. Bazzett HC: An analysis of the time-relationship of electrocardiograms. *Heart* 7:353–370, 1920
26. Fabiato A: Myoplasmic free calcium concentration reached during the twitch of an intact isolated cardiac cell and during calcium-induced release of calcium from the sarcoplasmic reticulum of a skinned cardiac cell from the adult rat or rabbit ventricle. *J Gen Physiol* 78:457–497, 1981
27. Stern MD, Capogrossi MC, Lakatta EG: Spontaneous calcium release from the sarcoplasmic reticulum in myocardial cells: mechanisms and consequences. *Cell Calcium* 9:247–256, 1988
28. Bers DM: Ca influx and sarcoplasmic reticulum Ca release in cardiac muscle activation during postrest recovery. *Am J Physiol* 248:H366–H381, 1985
29. Backx PH, Gao WD, Azan-Backx MD, Marban E: The relationship between contractile force and intracellular $[Ca^{2+}]$ in intact rat cardiac trabeculae. *J Gen Physiol* 105:1–19, 1995
30. Crespo LM, Grantham CJ, Cannell MB: Kinetics, stoichiometry and role of the Na-Ca exchange mechanism in isolated cardiac myocytes. *Nature* 345:618–621, 1990
31. Schannwell CM, Schneppenheim M, Perings S, Plehn G, Strauer BE: Left ventricular diastolic dysfunction as an early manifestation of diabetic cardiomyopathy. *Cardiology* 98:33–39, 2002
32. Bell DS: Diabetic cardiomyopathy: a unique entity or a complication of coronary artery disease? *Diabetes Care* 18:708–714, 1995
33. Maltsev VA, Vinogradova TM, Lakatta EG: The emergence of a general theory of the initiation and strength of the heartbeat. *J Pharmacol Sci* 100:338–369, 2006
34. Cooper GJ, Phillips AR, Choong SY, Leonard BL, Crossman DJ, Brunton DH, Saafi L, Dissanayake AM, Cowan BR, Young AA, Occleshaw CJ, Chan YK, Leahy FE, Keogh GF, Gamble GD, Allen GR, Pope AJ, Boyd PD,

Poppitt SD, Borg TK, Doughty RN, Baker JR: Regeneration of the heart in diabetes by selective copper chelation. *Diabetes* 53:2501–2508, 2004
35. Ren J, Davidoff AJ: Diabetes rapidly induces contractile dysfunctions in isolated ventricular myocytes. *Am J Physiol* 272:H148–H158, 1997
36. Cesario DA, Brar R, Shivkumar K: Alterations in ion channel physiology in diabetic cardiomyopathy. *Endocrinol Metab Clin North Am* 35:601–610, ix-x, 2006
37. Cannell MB, Berlin JR, Lederer WJ: Effect of membrane potential changes on the calcium transient in single rat cardiac muscle cells. *Science* 238:1419–1423, 1987
38. Yuan W, Ginsburg K, Bers DM: Comparison of sarcolemmal calcium channel current in rabbit and rat ventricular myocytes. *Journal of Physiology* 493:733–746, 1996
39. Malhotra A, Sanghi V: Regulation of contractile proteins in diabetic heart. *Cardiovasc Res* 34:34–40, 1997
40. Young LH, Dahl DM, Rauner D, Barrett EJ: Physiological hyperinsulinemia inhibits myocardial protein degradation in vivo in the canine heart. *Circ Res* 71:393–400, 1992
41. Depre C, Young ME, Ying J, Ahuja HS, Han Q, Garza N, Davies PJ, Taegtmeyer H: Streptozotocin-induced changes in cardiac gene expression in the absence of severe contractile dysfunction. *J Mol Cell Cardiol* 32:985–996, 2000
42. Candido R, Forbes JM, Thomas MC, Thallas V, Dean RG, Burns WC, Tikellis C, Ritchie RH, Twigg SM, Cooper ME, Burrell LM: A breaker of advanced glycation end products attenuates diabetes-induced myocardial structural changes. *Circ Res* 92:785–792, 2003